NIH Public Access
Author Manuscript
Biochemistry. Author manuscript; available in PMC 2011 July 6.

Published in final edited form as:
Biochemistry. 2010 July 6; 49(26): 5494–5503. doi:10.1021/bi100684g.

Cytidylyl- and Uridylyl Cyclase Activity of *Bacillus anthracis* Edema Factor and *Bordetella pertussis* CyaA

Martin Göttle, **Stefan Dove**, **Frieder Kees**, **Jens Schlossmann**, **Jens Geduhn**, **Burkhard König**, **Yuequan Shen**, **Wei-Jen Tang**, **Volkhard Kaever**, and **Roland Seifert**[1]
Department of Pharmacology and Toxicology (M.G., F.K., J.S.) and Department of Pharmaceutical and Medicinal Chemistry II (S.D.), Institute of Pharmacy, University of Regensburg, Germany; Institute of Organic Chemistry, University of Regensburg, Germany (J.G., B.K.); The College of Life Sciences, Nankai University, China (Y.S.); Ben May Department for Cancer Research, The University of Chicago (W.-J.T.); Institute of Pharmacology, Medical School of Hannover, Germany (V.K., R.S.).

Abstract

Cyclic adenosine 3′:5′-monophosphate (cAMP) and cyclic guanosine 3′:5′-monophosphate (cGMP) are second messengers for a numerous mammalian cell functions. The natural occurrence and synthesis of a third cyclic nucleotide (cNMP), cyclic cytidine 3′:5′-monophosphate (cCMP) is discussed controversially, and almost nothing is known about cyclic uridine 3′:5′-monophosphate (cUMP). *Bacillus anthracis* and *Bordetella pertussis* secrete the adenylyl cyclase (AC) toxins edema factor (EF) and CyaA, respectively, weakening immune responses and facilitating bacterial proliferation. A cell-permeable cCMP analog inhibits human neutrophil superoxide production. Here, we report that EF and CyaA also possess cytidylyl cyclase (CC) and uridylyl cyclase (UC) activity. CC- and UC activity was determined by a radiometric assay, using [α-^{32}P]CTP and [α-^{32}P]UTP as substrates, respectively, and by an HPLC method. The identity of cNMPs was confirmed by mass spectrometry. Based on available crystal structures, we developed a model illustrating conversion of CTP to cCMP by bacterial toxins. In conclusion, we have shown both EF and CyaA have a rather broad substrate-specificity and exhibit cytidylyl- and uridylyl cyclase activity. Both cCMP and cUMP may contribute to toxin actions.

Cyclic adenosine 3′:5′-monophosphate (cAMP) and cyclic guanosine 3′:5′-monophosphate (cGMP) are second messengers for numerous mammalian cell functions. The natural occurrence of a third cyclic nucleotide (cNMP), cyclic cytidine 3′:5′-monophosphate (cCMP), is discussed controversially. In 1974, Bloch *et al.* (1) observed that, in contrast to cAMP and cGMP, cCMP initiated the growth of leukemia L-1210 cells. In 1978, Cech and Ignarro (2) supposedly identified cCMP formation in mouse liver homogenate, but the methodology was problematic (3). The natural occurrence of cCMP in various mammalian organs was later suggested by fast atom bombardment (4), but follow-up studies have not yet been performed. A tentative cytidylyl cyclase (CC) activity was reported in various tissues (2–6), but the molecular identity of the responsible protein has not yet been elucidated. Moreover, cCMP-degrading phosphodiesterase activity was reported (7), but again, the identity of the responsible protein is elusive. Furthermore, ten proteins in brain tissue undergo phosphorylation following stimulation with cCMP (8,9), but the identity of the responsible protein kinase is unknown. cCMP may also modulate immune system

[1]Supported by the Deutsche Forschungsgemeinschaft (Graduiertenkolleg 760 "Medicinal Chemistry: Molecular Recognition - Ligand-Receptor Interactions" and research grant Se 529/5-2 to R.S.).

Corresponding author, Dr. Roland Seifert; Director, Institute of Pharmacology; Medical School of Hannover Carl-Neuberg-Str. 1, D-30625 Hannover, Germany; Tel: +49-511-532-2805, Fax: +49-511-532-4081; seifert.roland@mh-hannover.de.

NIH-PA Author Manuscript
NIH-PA Author Manuscript
NIH-PA Author Manuscript

NIH-PA Author Manuscript

NIH-PA Author Manuscript

NIH-PA Author Manuscript

functions. In macrophages, the cell-permeant cCMP-analog dibutyryl-cCMP inhibited thromboxane B_2 and leukotriene B_4 formation (10). In human neutrophils, dibutyryl-cCMP inhibited superoxide radical formation and the rise in cytosolic Ca^{2+} induced by a chemotactic peptide, resulting in neutrophil inactivation (11). Cyclic uridine 3′:5′-monophosphate (cUMP) was suggested to occur in mammalian cells as well (12), but almost nothing is known about a possible functional role of cUMP.

The causative agents of anthrax disease and whooping cough, *Bacillus anthracis* and *Bodetella pertussis*, respectively, exert their deleterious effects by the release of toxins (13,14). After interacting with surface receptors of eukaryotic host immune cells and translocation into the cytosol, the adenylyl cyclase (AC) toxins edema factor (EF) from *B. anthracis* and CyaA from *B. pertussis* bind to calmodulin (CaM), resulting in activation of catalysis (15,16). Both, EF and CyaA catalyze massive synthesis of cAMP. Consequently, immune cell function is inhibited rendering infection more severe (17–19).

Mammals express nine membranous AC isoforms (mACs 1–9) and a soluble AC. Serendipitously, we discovered 2′(3′)-*O*-(*N*-methylanthraniloyl)- (MANT)-substituted NTPs as competitive inhibitors of mACs and bacterial AC toxins (20–24). Additionally, PMEApp, the active metabolite of adefovir, a drug for the treatment of chronic hepatitis B virus infection, was identified as a potent inhibitor of EF and CyaA (25). Using crystallographic and molecular modeling approaches, we developed a three-site pharmacophore model for mAC and bacterial AC toxins, with binding domains for the base, the MANT-group and the polyphosphate chain (23,26). We resolved several EF and CyaA crystal structures and characterized the amino acids important for nucleotide binding and catalysis (16,27,28). Furthermore, we systematically examined the interactions of natural purine and pyrimidine nucleotides and MANT-substituted analogs with EF and CyaA in terms of catalysis, fluorescence changes and molecular modeling (26,29). Most surprisingly, MANT-CTP was the most potent competitive EF inhibitor among 16 compounds studied. Taken together, those studies revealed the catalytic sites of EF and CyaA to exhibit conformational flexibility and to accommodate both, purine and pyrimidine nucleotides. Those findings also raised the question whether in addition to ATP, other naturally occurring nucleotides, could be toxin substrates.

Materials and Methods

Chemicals and Biochemical Reagents

MANT-substituted nucleoside triphosphates (NTPs) of cytidine, inosine and uridine were synthesized as described (29). MANT-ATP, MANT-GTP were from Jena Bioscience, Jena, Germany. [α–^{32}P]ATP (800 Ci/mmol), [α–^{32}P]CTP (800 Ci/mmol) and [α–^{32}P]UTP (800 Ci/mmol) were purchased from PerkinElmer, Wellesley, MA. Aluminum oxide N Super 1 was purchased from MP Biomedicals, Eschwege, Germany. Acetonitrile (LC grade), ammonium acetate (p.A.), $CaCl_2$ dihydrate (p.A.), KCl (p.A.), methanol (LC grade), $MnCl_2$ tetrahydrate and $MgCl_2$ hexahydrate (highest quality), ortho-phosphoric acid (p.A.), sodium acetate (p.A.) and triethylamine were from Merck, Darmstadt, Germany. GTP·2 Na, ATP·2 Na and cAMP were purchased from Roche, Indianapolis, IN. cCMP·Na, cGMP·Na, cIMP·Na and cUMP·Na were from Biolog, Bremen, Germany. Bovine serum albumin (fraction V), 2′:3′-cCMP·Na, CMP·2 Na, CDP·3 Na, CTP·2 Na, EGTA, inosine, ITP·3 Na, UDP·Na, UMP·Na and UTP·3 Na dihydrate were purchased from Sigma-Aldrich, Seelze, Germany. Tris (ultrapure) was from USB, Cleveland, OH. [9-[2-(Phosphonomethoxy)ethyl]adenine diphosphate] (PMEApp) was supplied by Gilead Sciences, Foster City, CA. The full-length AC toxin edema factor (EF) from *B. anthracis* and the catalytic domain of *B. pertussis* AC protein (CyaA, amino acids 1 to 373) were

NIH-PA Author Manuscript

NIH-PA Author Manuscript

NIH-PA Author Manuscript

purified as described (15,30). Lyophilized calmodulin (CaM) from bovine brain was purchased from EMD Biosciences, Calbiochem, Darmstadt, Germany.

Isotopic Nucleotidyl Cyclase (NC) Activity Assay

For the determination of the potency of AC/CC inhibitors, assay tubes contained 10 μL of inhibitor at final concentrations from 1 nM to 100 μM and 20 μL of EF or CyaA dissolved in 75 mM Hepes·NaOH, pH 7.4, supplemented with 0.1% (m/v) bovine serum albumin to prevent protein adsorption. Final protein concentrations were 10 pM EF or CyaA (AC) and 30 pM (CC). Tubes were incubated for 2 min and reactions were initiated by the addition of 20 μL of reaction mixture consisting of the following components to yield the given final concentrations: 100 mM KCl, 5 mM free Mn^{2+}, 10 μM free Ca^{2+}, 100 μM EGTA, 100 μM cAMP and 100 nM CaM. In case of AC activity, ATP was added as non-labeled substrate at a final concentration of 40 μM and as radioactive tracer [α–^{32}P]ATP (0.2 μCi/tube). In case of CC activity, CTP was added as non-labeled substrate at 10 μM and as radioactive tracer [α–^{32}P]CTP (0.4 μCi/tube). Reactions were carried out for 10 min at 25°C (AC) and 20 min at 37°C (CC).

For the determination of K_m and k_{cat} values, assay tubes contained 10 μL of NTP/Mn^{2+} or NTP/Mg^{2+} and 20 μL of reaction mixture as described above. NTP/Mn^{2+} or NTP/Mg^{2+} (1 μM to 2 mM) plus 5 mM of free Mn^{2+} or Mg^{2+} were added. Reactions were initiated by the addition of 20 μL of EF or CyaA to yield the following final protein concentrations: 10 pM (EF and CyaA AC activities), 40 pM (EF and CyaA CC activities with Mn^{2+}) and 400 pM (EF CC activity with Mg^{2+} and UC activities). The amount of radioactive tracers was [α–^{32}P]ATP (0.2 μCi/tube), [α–^{32}P]CTP (0.8 μCi/tube) and [α–^{32}P]UTP (0.8 μCi/tube). Reactions were carried out for 10 min at 25°C (AC), 20 min at 37°C (CC) and 30 min at 37°C (UC). In saturation experiments using CTP/Mg^{2+} or UTP/Mn^{2+}, no extra non-labeled cNMPs was added to the reaction mixture. Saturation experiments using CTP/Mn^{2+} were performed in the presence of extra non-labeled cAMP or cCMP (100 μM each), and in the absence of cNMPs (without yielding significantly different results, data not shown). In saturation experiments using ATP/Mg^{2+} or CTP/Mg^{2+} on EF, 10 mM Tris/HCl were included in addition to the reaction mixture, and 1 mM EGTA and 400 nM free Ca^{2+} were used. In those experiments, the reaction mixture was incubated for 5 min at room temperature prior to the addition of CaM and again for 5 min after the addition of CaM in order to ensure the formation of steady-state equilibrium of complexing agents and divalent cations. Reactions were terminated by the addition of 20 μL of 2.2 N HCl, denaturated protein was sedimented by a 1-min centrifugation at 12,000 × g. [^{32}P]cNMP was separated from [α–^{32}P]NTP by transferring the samples to columns containing 1.4 g of neutral alumina. [^{32}P]cNMP was eluted by the addition of 4 mL 0.1 M ammonium acetate solution, pH 7.0 (31). Blank values were about 0.02% of the total amount of [α–^{32}P]NTP added; substrate turnover was < 3% of the total added [α–^{32}P]NTP. Samples were filled up with 10 mL Millipore water and Čerenkov radiation was measured in a PerkinElmer Tricarb 2800TR liquid scintillation analyzer. Free concentrations of divalent cations were calculated with WinMaxC (http://www.stanford.edu/~cpatton/maxc.html). K_i-values, K_m-values and k_{cat} -values were calculated using the Prism 4.02 software (Graphpad, San Diego, CA).

Non-Isotopic NC Assay and HPLC Analysis

In experiments using CyaA, reaction mixtures consisted of the following components to yield the given final concentrations in a total volume of 3 mL: 1 mM Mn^{2+}, 1 μM Ca^{2+}, 30 mM Hepes·NaOH, pH 7.4, 100 μM of the corresponding NTP and CaM at concentrations yielding 1:1 stoichiometry of CaM and bacterial cyclase toxin. In experiments using EF on CTP, UTP and ITP, reaction mixtures contained 5 mM Mn^{2+} and 5 μM Ca^{2+}. When EF was applied to GTP, Mn^{2+} was 1 mM and Ca^{2+} was 1 μM. Prior to the addition of enzyme, two

NIH-PA Author Manuscript

NIH-PA Author Manuscript

NIH-PA Author Manuscript

sample aliquots (300 μL each) were taken as negative controls: One sample aliquot was taken and stored on ice; a second sample aliquot lacking enzyme was taken and incubated in parallel with the reaction batch containing enzyme for 60 min at 37°C. Both, negative controls and reaction samples, later underwent the sample preparation process described subsequently. Assay tubes were incubated at 37°C for 4 min and reactions were initiated by the addition of 300 μL of EF or CyaA. Final protein concentrations ranged between 20 nM bacterial cyclase toxin and 20 nM CaM up to 1,500 nM bacterial cyclase toxin and 1,500 nM CaM as described in detail in "Results". Samples were taken at reaction times between 1 and 60 min. In order to achieve protein denaturation, sample aliquots (300 μL each) were added to 600 μL of acetonitrile and cooled to 4 °C . Threehundred μL of 40 μM inosine were added as internal standard (IS). Denatured protein was sedimented by a 1-min centrifugation at 12,000 × g. In order to achieve separation of the aqueous phase from the organic phase, samples were transferred into 5-mL-vials and 2 mL of dichloromethane were added. Samples were agitated for 20 min at 4 °C and centrifuged for 5 min at 1,000 × g. The aqueous phase was transferred into 1.5-mL-vials and stored at −80°C. Nucleotides were quantified using a Shimadzu LC10 HPLC system with the photometric detector set at 260 nm. A Phenomenex Synergi® Fusion-RP HPLC column (150 × 4.6 mm, 4 μm particle size, Phenomenex, Aschaffenburg, Germany) was eluted at 1 mL/min with a mobile phase consisting of 100 mM triethylamine with pH set to 6.6 using ortho-phosphoric acid. The mobile phase contained methanol at a concentration of 6% (v/v) in case of cCMP, cUMP and cIMP, 9% (v/v) in case of cGMP and 12% (v/v) in case of cAMP. The mobile phase was run at 1 mL/min, the temperature of the column oven was 35°C and the injection volume was 5 μL. Chromatograms were evaluated using external standardization and Shimadzu LC solution 1.22 SP1 software.

Mass Spectrometry

LC-MS/MS was performed using an Agilent 1100 HPLC system and a TSQ-7000 Thermoquest Finnigan triple quadrupol mass spectrometer. A Phenomenex Luna C18 Aqua HPLC column (150 × 2 mm, 3 μm particle size) was eluted with the mobile phase at 0.3 mL/min using a gradient of 0.1% formic acid (A) and acetonitrile (B) with 0% B (v/v, min 0 to 2), 80% B (v/v, min 2 to 15), 80% B (v/v, min 15 to 20), 0% B (v/v, min 20 to 25) and 0% B (v/v, min 25 to 35). The autosampler system was cooled to 5°C, the temperature of the column oven was 40°C and the injection volume was 20 μL. Upon ESI (capillary temperature 250 °C, ESI spray voltage 4 kV), argon was used for collision-induced dissociation with collision energies of 25 V (cCMP), 15 V (cUMP) and 20 V (cIMP). Selective reaction monitoring (SRM) in positive mode was performed monitoring m/z transitions of 306.0 to 112.2 (cCMP), of 324.2 to 307.0 (cUMP) and of 330.9 to 137.2 (cIMP). Data were interpreted using the Xcalibur 3.1 software.

Models of EF and CyaA in Complex with ATP and CTP

The models are based on the crystal structures of EF in complex with 3'-deoxy-ATP, PDB 1xfv (28) and CyaA in complex with PMEApp, PDB 1zot (16), respectively. Docking studies were performed with the molecular modeling suite SYBYL 7.3 (Tripos, L. P., St. Louis, MO) on a Silicon Graphics Octane workstation. ATP and CTP were manually docked to both enzymes in a conformation similar to that of 3'-deoxy-ATP bound to EF. Hydrogens were added to the proteins and the water molecules and the complexes were provided with AMBER_FF99 charges. The models were refined with the AMBER_FF99 force field (32) (distant dependent dielectric constant ε = 4,25 cycles steepest descent, followed by Powell conjugate gradient, end gradients of 0.01 kcal $mole^{-1}$ $Å^{-1}$).

NIH-PA Author Manuscript

NIH-PA Author Manuscript

NIH-PA Author Manuscript

Results

Isotopic NC Activity Assay

Incubation of 20 pM EF with 0.4 μCi/tube [α–^{32}P]CTP and 10 μM unlabeled CTP in the presence of 5 mM Mn^{2+} followed by alumina solid phase extraction and liquid scintillation analysis resulted in a pronounced signal increasing linearly over time (Fig. **1A**). Blank values were generally < 0.02% of the total added amount of [α–^{32}P]CTP indicating full retention of [α–^{32}P]CTP on the column matrix during extraction. By increasing the enzyme concentration, the resulting signal increased proportionally (Fig. **1B**). As shown in Fig. **1C**, the signal intensity showed considerable dependence on pH with the highest intensity obtained at physiological pH values and poor intensities at low pH values (pH 6.0) or high pH values (pH 9.0). At pH 5.0, no conversion of [α–^{32}P]CTP took place. CaM activated cCMP formation with EC_{50} values of 670 ± 50 pM in case of EF (Fig. **1D**) and 80 ± 5 pM in case of CyaA (data not shown). In the absence of CaM, 40 pM EF increased the signal 3-fold compared with blank values. Similar results were obtained with CyaA (data not shown).

Solid Phase Extraction of cCMP and cUMP and HPLC Analysis

In order to ensure complete retention of the starting material [α–^{32}P]NTP on alumina columns during solid phase extraction and to determine recovery values for [^{32}P]cNMP, mixtures of non-labeled nucleotides were subjected to solid phase extraction (SPE) and HPLC analysis. Prior to SPE, HPLC chromatograms from nucleotide mixtures show peaks from 15 μM CMP, CDP, CTP and 3′:5′-cCMP (Fig. **2A**, dashed line) as well as from 15 μM UMP, UDP, UTP and 3′:5′-cUMP (Fig. **2B**, dashed line). After SPE, 3′:5′-cCMP and 3′:5′-cUMP were eluted while the signals from acyclic nucleotides were missing. The recovery values were 70% in case of 3′:5′-cCMP and 50% in case of 3′:5′-cUMP. Therefore, the SPE procedure used in this work completely retained acyclic nucleotides on the alumina columns while cyclic pyrimidine nucleotides were eluted. Thus, the signals detected by liquid scintillation in the isotopic NC assay can only result from cNMPs; non-specific signals from acyclic nucleotides can be excluded.

In order to ensure that the cNMPs formed enzymatically were of 3′:5′-cNMP structure and not of the also naturally occurring 2′:3′-cNMP structure, we applied 15 μM 3′:5′-cCMP and 2′:3′-cCMP to SPE and HPLC analysis. As shown in Fig. **2C**, a peak from 2′:3′-cCMP at a retention time of 3.3 min was detected while the retention time of 3′:5′-cCMP was 8.2 min. Both nucleotides were eluted in SPE with recoveries of about 70%. Therefore, 3′:5′-cNMP and 2′:3′-cNMP isomers could easily be discriminated based on their retention times, and cNMPs with 2′:3′-cNMP structure were never detected in enzymatic reactions within this project.

Enzyme Kinetics

Fig. **3** shows the results of substrate saturation experiments using the isotopic NC activity assay with CTP/Mn^{2+} or UTP/Mn^{2+} on EF or CyaA; an overview of the kinetic properties of the AC activities, CC activities and UC activities of EF and CyaA is given in Table **1**. Using Mn^{2+}, the K_m value of EF CC activity was 3-fold lower than the K_m value of EF AC activity. The K_m value of EF UC activity was 4-fold higher than the value of AC activity. Using Mg^{2+}, the K_m value of EF CC activity was 2-fold higher than the value of AC activity. Using CyaA and Mn^{2+} yielded similar K_m values in case of AC, CC and UC activity. Enzyme activities decreased in the order AC > CC > UC (k_{cat} values). Various free Ca^{2+} concentrations between 100 nM – 100 μM did not change this substrate-specificity (data not shown). It should also be noted that we determined AC activity on one hand and CC- and UC activities on the other hand at different temperatures (see Materials and Methods), introducing some bias in data interpretation. However, these different

NIH-PA Author Manuscript

NIH-PA Author Manuscript

NIH-PA Author Manuscript

experimental conditions were necessary to avoid substrate depletion with ATP as substrate and ensure sufficiently sensitive detection of product formation with CTP and UTP. Using Mn^{2+}, the k_{cat} value of EF CC activity was 57-fold lower than the value of AC activity, and UC activity was even 4-fold lower than CC activity. Using CyaA and Mn^{2+}, the k_{cat} value of CC activity was 37-fold lower than compared to the value of AC activity, and UC activity was even 30-fold lower than CC activity. However, the isotopic assay was sensitive enough to detect even those low enzyme activities. Table **1** also shows the different catalytic efficiencies of EF and CyaA NC reactions given as $k_{cat} \cdot K_m^{-1}$ [$M^{-1} \cdot s^{-1}$]. Using Mn^{2+}, EF CC activity is 20-fold less efficient as compared to EF AC activity and EF UC activity is even ~800-fold less efficient. Using CyaA, similar data were obtained (Table **1**).

Inhibition of NC Activity

EF and CyaA CC activity was inhibited using standard AC inhibitors. Using Mn^{2+}, PMEApp (25) inhibited EF AC activity with a K_i value of 2.0 ± 0.5 nM, while PMEApp inhibited CC activity with a K_i value of 4.5 ± 0.4 nM. The K_i values of PMEApp on CyaA were 1.0 ± 0.3 nM (AC activity) and 1.1 ± 0.02 nM (CC activity). The K_i values of five MANT-substituted nucleotides on EF and CyaA AC and CC activities are given in Table **2**. MANT-CTP was found to be the most potent MANT-nucleotide on EF AC and CC activity, yielding similar K_i values. MANT-ATP inhibited EF CC activity with about 7-fold lower potency than MANT-CTP, followed by MANT-GTP, MANT-UTP and MANT-ITP. The order of potency of MANT-nucleotides on CyaA CC activity was MANT-ITP > MANT-CTP > MANT-UTP > MANT-ATP > MANT-GTP. On EF and CyaA, the K_i values of AC and CC inhibition showed significant correlation (Fig. **4**), indicating that CC- and AC activities originated from a single catalytic site.

Non-Isotopic NC Assay and HPLC Analysis

EF and CyaA were incubated with several NTPs, and the formation of the corresponding cNMPs was analyzed. Fig. **5** shows HPLC chromatograms of reaction samples taken after reaction times between 0 min and 60 min. The chromatogram of the incubation of 20 nM EF with 100 μM CTP at a reaction time of 0 min (Fig. **5A**, purple line) showed a peak resulting from the starting material CTP at a retention time of 3.8 min while the internal standard (IS) inosine (40 μM) gave a peak at 5.7 min; no additional peaks were detected for 0 min reaction time at retention times of 6 min to 10 min. With increasing reaction time, the CTP peak at a retention time of 3.8 min decreased, while at a retention time of 8.3 min, a new peak was detected. This peak increased proportionally to the decrease of the CTP peak. This newly detected signal at a retention time of 8.3 min exhibited an identical retention time as 3′:5′-cCMP applied as external standard (Fig. **5A**, dashed line). At different reaction times, the internal standard (inosine, 40 μM) yielded constant signals at a retention time of 5.7 min ensuring reproducible nucleotide recoveries.

In order to answer the question which NTP is converted preferentially by EF, ATP or CTP, both NTPs (100 μM each) were incubated simultaneously with 1 nM EF and 1 nM CaM in one reaction vial, allowing competition of ATP and CTP for the catalytic site. ATP turned out to be converted preferentially, e.g. after 2 h of incubation at 37°C, the turnover was about 90% for ATP and about 10% for CTP (data not shown). When 120 nM EF were incubated with 100 μM UTP, chromatograms showed the UTP signal at a retention time of 4.9 min (Fig. **5B**, purple line). With increasing reaction time, a decrease of the UTP signal was observed, and at a retention time of 10.8 min, a new signal was detected exhibiting the identical retention time as 20 μM 3′:5′-cUMP applied as external standard (Fig. **5B**, dashed line). Similarly, upon incubation of 100 μM ITP with 300 nM EF (Fig. **5C**), a decrease of the ITP peak at a retention time of 6.2 min was observed while a new peak increased at a

NIH-PA Author Manuscript

NIH-PA Author Manuscript

NIH-PA Author Manuscript

retention time of 14.2 min, exhibiting the identical retention time as 3′:5′-cIMP applied as external standard (Fig. **5C**, dashed line).

In order to ensure that the observed NTP conversions resulted from specific enzymatic activity, 20 nM EF and 100 μM CTP were incubated similarly to the experiment shown in Fig. **5A**, and for comparison, 20 nM of heat-inactivated EF were incubated with 100 μM CTP. After 60 min of incubation using EF, the CTP peak at a retention time of 3.8 min had been converted to a signal at 8.3 min exhibiting the retention time of cCMP external standard (Fig. **5D**, solid line). The chromatogram resulting from an incubation of 60 min using heat-inactivated EF showed no new peak from cCMP at a retention time of 8.3 min, but the peak from the starting material CTP persisted at a retention time of 3.8 min (Fig. **5D**, dashed line). Thus, no conversion of CTP was detected using heat-inactivated enzyme.

HPLC chromatograms shown in Fig. **5** were used to calculate nucleotide concentrations and to depict NTP conversion to cNMP by EF with increasing reaction time (Fig. **6**). EF concentrations were adjusted according to the efficiency of conversion of the individual NTPs. With 20 nM EF, 120 nM EF and 500 nM EF, respectively, complete conversion of 100 μM CTP, UTP and ITP occurred within 60 min. When 500 nM EF were incubated with 100 μM GTP, chromatograms showed a decrease of the signal from GTP and a new signal exhibiting the retention time of standard cGMP (data not shown). However, although the EF concentration was high (500 nM), the turnover of GTP within a reaction time of 60 min was 13% only, showing inferior enzymatic activity of EF on GTP as compared to CTP, UTP and ITP. When CyaA was used instead of EF, similar chromatographic results were obtained (data not shown). Chromatograms also showed complete conversion of CTP, UTP and ITP within 60 min yielding peaks at retention times of the corresponding cNMP standards. CyaA concentrations needed for complete turnover of 100 μM NTP within 60 min were 30 nM (CTP), 600 nM (UTP) and 1,500 nM (ITP). When 1,500 nM CyaA were applied to 100 μM GTP, the turnover within 60 min was 90%.

Mass Spectrometry

In order to ensure the exact identities of the cNMP products from enzymatic reactions, samples were applied to LC-MS/MS and the resulting data were compared to results from cNMP standards. Fig. **7** shows mass spectra and chromatograms from SRM for cCMP (A–C), cUMP (D–F) and cIMP (G–I). The mass spectrum of cCMP (Fig. **7A**) shows signals from protonated cCMP (m/z = 306.0) and from the protonated cytosine base (m/z = 112.2). Selective reaction monitoring of the m/z transition of 306.0 to 112.2 proofed the existence of cCMP in the nucleotide standard (Fig. **7B**) as well as in samples from the enzymatic reaction of EF with CTP (Fig. **7C**). In case of cUMP, mass signals resulted from the protonated cUMP molecule (m/z = 307.0), the cUMP-ammonia adduct (m/z = 324.2) and the protonated uracil base (m/z = 113.3) (Fig. **7D**). SRM of the m/z transition of 324.2 to 307.0 proofed the existence of cUMP in the nucleotide standard (Fig. **7E**) and in reaction samples (Fig. **7F**). The mass spectrum of cIMP (Fig. **7G**) shows signals from protonated cIMP (m/z = 330.9) and from the protonated hypoxanthine base (m/z = 137.2). As determined by SRM of the m/z transition of 330.9 to 137.2, cIMP was found in nucleotide standard and reaction sample (Fig. **7H–I**).

Modeling of the Nucleotide Binding Modes

The crystal structures of EF in complex with 3'-deoxy-ATP, PDB 1xfv (28) and CyaA in complex with PMEApp, PDB 1zot (16) were used for docking of ATP and CTP (Fig. **8**). The nucleotide binding site of EF is a spacious cavity located at the interface of two structural domains, C_A (D294 – N349, A490 – K622) and C_B (V350 – T489). The position of two Mg^{2+} ions, one coordinated by D491, D493 and H577, the other by the α-, β- and γ-

NIH-PA Author Manuscript

NIH-PA Author Manuscript

NIH-PA Author Manuscript

phosphates of the substrates, indicates two-metal-ion catalysis starting with a nucleophilic attack of the deprotonated 3'-oxygen on the a-phosphorus (28). Molecular dynamics simulations suggested that this attack is facilitated by a 3'-endo conformation of the ribosyl moiety, by direct coordination of the 3'-oxygen by the metal, and by the activation of a water molecule by H351 leading to deprotonization of the 3'-OH group (28). Fig. **8 (A, B)** compares the EF binding modes of ATP and CTP. No differences are obvious in the triphosphate and the ribosyl regions. The triphosphate groups are cyclically folded due to the coordination by Mg^{2+}. The β- and the γ-phosphates form additional salt bridges with K346, K353 and K372. The ribosyl moieties adopt 3'-endo conformations and contact the side chains of L348 and H577. Moreover, electrostatic interactions between the ring oxygens and the amide NH_2 of N583 are possible. The 3'-oxygen atoms are about 3.4 Å distant from both Mg^{2+} ions.

The nucleotide bases of ATP and CTP fit to the same pocket mainly consisting of amino acids of the EF switch B (G578 – N591). The interactions equal those described for the corresponding MANT-ATP and MANT-CTP derivatives (29). The amino groups of adenine and cytosine form the same two hydrogen bonds with the backbone oxygens of T548 and T579, and the ring planes are aligned with the side chain of N583. Differences in ATP and CTP binding are not only due to the greater van der Waals surface of ATP (by ~22 $Å^2$). In the presence of Mn^{2+}, MANT-CTP is a ~6 times more potent EF inhibitor than its ATP analogue (29). A possible reason for the higher affinity may be a water molecule in an ideal position where it forms three hydrogen bonds, bridging the cytosine oxygen with the side chains of R329 and E580 (Fig. **8B**).

The interactions of ATP and CTP with CyaA are very similar to those with EF. An alignment of the nucleotide binding sites of both enzymes, performed by superposition of the backbone atoms of 15 amino acids surrounding the ligands (rms distance 1.22 Å), illustrates the close correspondence (see Fig. **8C**). 14 of the 15 residues are identical, only EF-T548 is replaced by CyaA-V271. Fig. **8D** shows the putative interactions of CyaA with CTP. Including the postulated water molecule bridging the cytosine oxygen with the side chains of R41 and E301 and the two hydrogen bonds of the amino group with the backbone oxygens of V271 and T300, all of the CTP-EF interactions are principally reproduced. CyaA-H298 adopts a different rotational state compared to EF-H377, since the side chain of H398 is not coordinated to a metal ion in the crystal structure, enabling the imidazole NH to form an additional hydrogen bond with the cytosin oxygen in the minimized model. In the case of CyaA-ATP binding, the complete pattern of EF-ATP interactions can be reproduced (not shown).

Discussion

Our present study clearly demonstrates that the “AC” toxins EF and CyaA do not only catalyze the formation of cAMP, but also the formation of cCMP, cUMP and cIMP. These multiple cNMP-forming enzyme activities originate from a single catalytic site. Considering the previously reported broad base-specificities of the two toxins (21,26,29), our data are not totally unexpected. The development of the cCMP field had been seriously hampered by methodological problems (2,3). In our present study we describe straight-forward radiometric and HPLC-based methods to assess cNMP formation. The sensitive and simple radiometric method described herein can be applied in any biochemical laboratory without specialized equipment. The HPLC method can be used to prepare isotopically labeled cNMPs as standards for mass spectrometry that are not commercially available.

The substrate saturation experiments show some intriguing differences between the results with Mn^{2+} and Mg^{2+}. Generally, the k_{cat} values of EF-AC and EF-CC activity are similar

NIH-PA Author Manuscript

NIH-PA Author Manuscript

NIH-PA Author Manuscript

and rather independent of the cation, but K_m is by a factor of ~5 (AC) and ~34 (CC), respectively, lower in the case of Mn^{2+}. Thus, not the enzyme mechanism, but the substrate affinity is mainly affected by the cation species. Additionally, the K_m value of CTP is 3-fold lower than that of ATP with Mn^{2+}, but more than 2-fold higher compared to ATP with Mg^{2+}. This corresponds to our previous findings that the affinities of MANT-CTP at CyaA (26) and EF (29) were significantly higher than those of MANT-ATP only if Mn^{2+} was used as divalent cation. These discrepancies are probably not due to different direct interactions of the substrates or the products with the cations since the binding constants of UTP and PP_i, respectively, for Mg^{2+} and Mn^{2+} are very similar (35). Therefore, the reasons for higher nucleotide affinity with Mn^{2+} as cofactor should rely on interactions within the enzyme-substrate complex. However, if one compares the mean Mg^{2+}-O distances of the structures used for modeling, EF in complex with 3'-deoxy-ATP (2.47 ± 0.22) (28) and CyaA in complex with PMEApp (2.30 ± 0.34) (16), with the mean Mn^{2+}-O distance (2.53 ± 0.18) in the highest resolution AC structure with Mn^{2+} (PDB 1ybu, (36), it becomes obvious that different cation-oxygen distances do not play an essential role. Probably, an exchange of the cation species will induce subtle rearrangements of the catalytic site in the enzyme-substrate complex which mainly affect the binding affinity of CTP. This "fine tuning" is not obvious from the present crystal structures with limited resolution, but can, if at all, only be analyzed by *ab-initio* quantum chemical calculations. Similar differences between Mn^{2+} and Mg^{2+} exist also in the case of mACs (37). Compared to Mg^{2+}, Mn^{2+} significantly reduces the K_m value of ATP and increases the inhibitory potency of a substrate analog, but is of lower influence on V_{max}.

In our previous studies, we characterized the interactions of the catalytic sites of EF and CyaA with various purine and pyrimidine NTPs and MANT-NTPs (26,29). We developed a three-site pharmacophore model for mAC, EF and CyaA attributing major importance to the MANT substituent for nucleotide affinity, followed by the phosphate tail (23). The higher affinity of MANT-NTPs is a result from additional hydrophobic interactions of the MANT-group with F586 in EF and F306 in CyaA, respectively (26,29). The base turned out to play a minor role as the catalytic site of AC is spacious and conformationally flexible and accommodates various purine and pyrimidine nucleotides (26,29). Using kinetic FRET competition experiments, we have shown that MANT-ATP and MANT-CTP reversibly bind to the catalytic site of EF, further corroborating a single catalytic site in EF (29). The binding modes suggested for the bases in MANT-ATP and MANT-CTP are the same as in the case of ATP and CTP, respectively (see Fig. **8**). The affinity of CTP and MANT-CTP may be especially due to the possibility that a water molecule mediates a network of hydrogen bonds between the cytosine oxygen and the side chains of R329 and E580. Taken together, these results confirm that various bases, in particular adenine and cytosine, can be accommodated by the EF catalytic site. Also in the case of CyaA, modeling of the binding modes of MANT-NTPs indicated that all bases are aligned in similar positions (26). ATP, CTP and their MANT derivatives can form the same interactions with EF and CyaA. However, the K_m value of UTP for EF is 4-fold higher than that of ATP, whereas the affinities of the purines MANT-GTP and MANT-ATP as well as of the pyrimidines MANT-UTP, MANT-ITP and MANT-CTP for CyaA are similar. A possible reason is that EF-D582 corresponds to CyaA-N303. After a slight change of the rotamer state of the asparagine side chain, the amide may serve as hydrogen donor for the carbonyl oxygens in the purine-6 and pyrimidine-4 positions, respectively. Collectively, our studies demonstrate broad base-specificity of the catalytic sites of EF and CyaA both in terms of substrates and inhibitors.

Our data on CC- and UC activities of bacterial toxins have important implications for the cNMP field in general. Taking into consideration the fact that bacterial “AC” toxins, mACs and sGC all exhibit broad-base-specificity (21–24,38), the question arises whether mammalian NCs synthesize cCMP and cUMP as well. The analysis of this issue is not

NIH-PA Author Manuscript

NIH-PA Author Manuscript

NIH-PA Author Manuscript

trivial since the catalytic activities of mammalian NCs are much lower than those of bacterial toxins. Hence, the sensitivity of the radiometric method described in this report may not be sufficient to detect such activities. To improve sensitivity we are currently developing highly sensitive mass spectrometry methods for quantitative detection of cNMPs. To this end, we have studied whether sGC and mACs exhibit UC activity using the radiometric approach. In fact, sGC exhibits nitric oxide-stimulated UC activity, whereas for recombinant mACs 2 and 5 expressed in Sf9 insect cell membranes no UC activity was detected (21). This is quite remarkable since the affinity of all these NCs for inhibitory UTP- and CTP analogs is quite similar (38). These data are a first indication that CC- and UC activities of bacterial and mammalian NCs do not simply represent "substrate leakiness" but reflect as yet poorly understood functional differences between the various cNMPs. Almost nothing is known about a possible functional role of cUMP. As the cell-permeant cCMP-analog dibutyryl-cCMP blunts host immune responses (10,11), we hypothesize that the formation of cCMP by EF and CyaA synergizes with cAMP to disrupt immune responses. Finally, our data urgently call for an in-depth analysis of the substrate-specificity of mammalian NCs with the methods described in this report or even more sensitive mass spectrometry methods.

Abbreviations

AC	adenylyl cyclase
CaM	calmodulin
CC	cytidylyl cyclase
cNMP	cyclic nucleoside 3′,5′-monophosphate
EF	edema factor
IC	inosinylyl cyclase
IS	internal standard
LC	liquid chromatography
MANT	methylanthraniloyl-
mAC	membranous mammalian AC
NC	nucleotidyl cyclase
NTP	nucleoside 5′-triphosphate
PMEApp	[9-[2-(phosphonomethoxy)ethyl]adenine diphosphate]
RT	retention time
sGC	soluble guanylyl cyclase
SPE	solid phase extraction
SRM	selective reaction monitoring
UC	uridylyl cyclase

Acknowledgments

We thank Mrs. Susanne Brüggemann, Mr. Josef Kiermeier and Mrs. Astrid Seefeld for expert technical assistance. Thanks are also due to the reviewers for their constructive critique.

NIH-PA Author Manuscript

NIH-PA Author Manuscript

NIH-PA Author Manuscript

References

1. Bloch A, Dutschman G, Maue R. Cytidine 3′,5′-monophosphate (cyclic CMP). II. Initiation of leukemia L-1210 cell growth *in vitro*. Biochem. Biophys. Res. Commun. 1974; 59:955–959. [PubMed: 4369899]
2. Cech SY, Ignarro LJ. Cytidine 3′,5′-monophosphate (cyclic CMP) formation by homogenates of mouse liver. Biochem. Biophys. Res. Commun. 1978; 80:119–125. [PubMed: 23778]
3. Gaion RM, Krishna G. Cytidylate cyclase: The product isolated by the method of Cech and Ignarro is not cytidine 3′,5′-monophosphate. Biochem. Biophys. Res. Commun. 1979; 86:105–111. [PubMed: 435290]
4. Newton RP, Salih SG, Salvage BJ, Kingston EE. Extraction, purification and identification of cytidine 3′,5′-cyclic monophosphate from rat tissues. Biochem. J. 1984; 221:665–673. [PubMed: 6089744]
5. Newton RP, Salvage BJ, Hakeem NA. Cytidylate cyclase: Development of assay and determination of kinetic properties of a cytidine 3′,5′-cyclic monophosphate-synthesizing enzyme. Biochem. J. 1990; 265:581–586. [PubMed: 2154193]
6. Newton RP, Groot N, van Geyschem J, Diffley PE, Walton TJ, Bayliss MA, Harris FM, Games DE, Brenton AG. Estimation of cytidylyl cyclase activity and monitoring of side-product formation by fast-atom bombardment mass spectrometry. Rapid Commun. Mass Spectrom. 1997; 11:189–194. [PubMed: 9050266]
7. Newton RP, Bayliss MA, Khan JA, Bastani A, Wilkins AC, Games DE, Walton TJ, Brenton AG, Harris FM. Kinetic analysis of cyclic CMP-specific and multifunctional phosphodiesterases by quantitative positive-ion fast-atom bombardment mass spectrometry. Rapid Commun. Mass Spectrom. 1999; 13:574–584. [PubMed: 10230067]
8. Bond AE, Dudley E, Tuytten R, Lemiere F, Smith CJ, Esmans EL, Newton RP. Mass spectrometric identification of rab23 phosphorylation as a response to challenge by cytidine 3′,5′-cyclic monophosphate in mouse brain. Rapid Commun. Mass Spectrom. 2007; 21:2685–2692. [PubMed: 17639578]
9. Ding S, Bond AE, Lemiere F, Tuytten R, Esmans EL, Brenton AG, Dudley E, Newton RP. Online immobilized metal affinity chromatography/mass spectrometric analysis of changes elicited by cCMP in the murine brain phosphoproteome. Rapid Commun. Mass Spectrom. 2008; 22:4129–4138. [PubMed: 19023864]
10. Elliott GR, Lauwen AP, Bonta IL. Dibutyryl cytidine 3′:5′-cyclic monophosphate; an inhibitor of A23187-stimulated macrophage leukotriene B_4 synthesis. Agents Actions. 1991; 32:90–91. [PubMed: 1647653]
11. Ervens J, Seifert R. Differential modulation by N^4, 2′-*O*-dibutyryl cytidine 3′:5′-cyclic monophosphate of neutrophil activation. Biochem. Biophys. Res. Commun. 1991; 174:258–267. [PubMed: 1703410]
12. Newton RP, Kingston EE, Hakeem NA, Salih SG, Beynon JH, Moyse CD. Extraction, purification, identification and metabolism of 3’,5’-cyclic UMP, 3’,5’-cyclic IMP and 3’,5’-cyclic dTMP from rat tissues. Biochem. J. 1986; 236:431–439. [PubMed: 3019316]
13. Ahuja N, Kumar P, Bhatnagar R. The adenylate cyclase toxins. Crit. Rev. Microbiol. 2004; 30:187–196. [PubMed: 15490970]
14. Ladant D, Ullmann A. *Bordetella pertussis* adenylate cyclase: A toxin with multiple talents. Trends. Microbiol. 1999; 7:172–176. [PubMed: 10217833]
15. Drum CL, Yan SZ, Sarac R, Mabuchi Y, Beckingham K, Bohm A, Grabarek Z, Tang WJ. An extended conformation of calmodulin induces interactions between the structural domains of adenylyl cyclase from *Bacillus anthracis* to promote catalysis. J. Biol. Chem. 2000; 275:36334–36340. [PubMed: 10926933]
16. Guo Q, Shen Y, Lee YS, Gibbs CS, Mrksich M, Tang WJ. Structural basis for the interaction of *Bordetella pertussis* adenylyl cyclase toxin with calmodulin. EMBO J. 2005; 24:3190–3201. [PubMed: 16138079]

NIH-PA Author Manuscript

NIH-PA Author Manuscript

NIH-PA Author Manuscript

17. Hewlett EL, Donato GM, Gray MC. Macrophage cytotoxicity produced by adenylate cyclase toxin from *Bordetella pertussis*: More than just making cyclic AMP! Mol. Microbiol. 2006; 59:447–459. [PubMed: 16390441]

18. Paccani SR, Tonello F, Ghittoni R, Natale M, Muraro L, D′Elios MM, Tang WJ, Montecucco C, Baldari CT. Anthrax toxins suppress T lymphocyte activation by disrupting antigen receptor signalling. J. Exp. Med. 2005; 201:325–331. [PubMed: 15699068]

19. Tournier JN, Quesnel-Hellmann A, Mathieu J, Montecucco C, Tang WJ, Mock M, Vidal DR, Goossens PL. Anthrax edema toxin cooperates with lethal toxin to impair cytokine secretion during infection of dendritic cells. J. Immunol. 2005; 174:4934–4941. [PubMed: 15814721]

20. Johnson RA, Shoshani I. Inhibition of *Bordetella pertussis* and *Bacillus anthracis* adenylyl cyclases by polyadenylate and "P"-site agonists. J. Biol. Chem. 1990; 265:19035–19039. [PubMed: 2121733]

21. Gille A, Lushington GH, Mou TC, Doughty MB, Johnson RA, Seifert R. Differential inhibition of adenylyl cyclase isoforms and soluble guanylyl cyclase by purine and pyrimidine nucleotides. J. Biol. Chem. 2004; 279:19955–19969. [PubMed: 14981084]

22. Mou TC, Gille A, Fancy DA, Seifert R, Sprang SR. Structural basis for the inhibition of mammalian membrane adenylyl cyclase by 2′(3′)-*O*-(*N*-Methylanthraniloyl)-guanosine 5′-triphosphate. J. Biol. Chem. 2005; 280:7253–7261. [PubMed: 15591060]

23. Mou TC, Gille A, Suryanarayana S, Richter M, Seifert R, Sprang SR. Broad specificity of mammalian adenylyl cyclase for interaction with 2′,3′-substituted purine- and pyrimidine nucleotide inhibitors. Mol. Pharmacol. 2006; 70:878–886. [PubMed: 16766715]

24. Gille A, Seifert R. 2′(3′)-*O*-(*N*-methylanthraniloyl)-substituted GTP analogs: A novel class of potent competitive adenylyl cyclase inhibitors. J. Biol. Chem. 2003; 278:12672–12679. [PubMed: 12566433]

25. Shen Y, Zhukovskaya NL, Zimmer MI, Soelaiman S, Bergson P, Wang CR, Gibbs CS, Tang WJ. Selective inhibition of anthrax edema factor by adefovir, a drug for chronic hepatitis B virus infection. Proc. Natl. Acad. Sci. USA. 2004; 101:3242–3247. [PubMed: 14978283]

26. Göttle M, Dove S, Steindel P, Shen Y, Tang WJ, Geduhn J, König B, Seifert R. Molecular analysis of the interaction of *Bordetella pertussis* adenylyl cyclase with fluorescent nucleotides. Mol. Pharmacol. 2007; 72:526–535. [PubMed: 17553924]

27. Drum CL, Yan SZ, Bard J, Shen YQ, Lu D, Soelaiman S, Grabarek Z, Bohm A, Tang WJ. Structural basis for the activation of anthrax adenylyl cyclase exotoxin by calmodulin. Nature. 2002; 415:396–402. [PubMed: 11807546]

28. Shen Y, Zhukovskaya NL, Guo Q, Florian J, Tang WJ. Calcium-independent calmodulin binding and two-metal-ion catalytic mechanism of anthrax edema factor. EMBO J. 2005; 24:929–941. [PubMed: 15719022]

29. Taha HM, Schmidt J, Göttle M, Suryanarayana S, Shen Y, Tang WJ, Gille A, Geduhn J, König B, Dove S, Seifert R. Molecular analysis of the interaction of anthrax adenylyl cyclase toxin, edema factor, with 2′(3′)-*O*-(*N*-(methyl)anthraniloyl)-substituted purine and pyrimidine nucleotides. Mol. Pharmacol. 2009; 75:693–703. [PubMed: 19056899]

30. Drum CL, Shen Y, Rice PA, Bohm A, Tang WJ. Crystallization and preliminary X-ray study of the edema factor exotoxin adenylyl cyclase domain from *Bacillus anthracis* in the presence of its activator, calmodulin. Acta Crystallogr. D Biol. Crystallogr. 2001; 57:1881–1884. [PubMed: 11717504]

31. Alvarez R, Daniels DV. A single column method for the assay of adenylate cyclase. Anal. Biochem. 1990; 187:98–103. [PubMed: 2164795]

32. Cornell WD, Cieplak P, Bayly CI, Gould IR, Merz KMJ, Ferguson DM, Spellmeyer DC, Fox T, Caldwell JW, Kollman PA. A second generation force field for the simulation of proteins and nucleic acids. J. Am. Chem. 1995; 117:5179–5197.

33. Bouhss A, Vincent M, Munier H, Gilles AM, Takahashi M, Barzu O, Danchin A, Gallay J. Conformational transitions within the calmodulin-binding site of *Bordetella pertussis* adenylate cyclase studied by time-resolved fluorescence of W242 and circular dichroism. Eur. J. Biochem. 1996; 237:619–628. [PubMed: 8647105]

NIH-PA Author Manuscript

NIH-PA Author Manuscript

NIH-PA Author Manuscript

34. Glaser P, Munier H, Gilles AM, Krin E, Porumb T, Barzu O, Sarfati R, Pellecuer C, Danchin A. Functional consequences of single amino acid substitutions in calmodulin-activated adenylate cyclase of *Bordetella pertussis*. EMBO J. 1991; 10:1683–1688. [PubMed: 2050107]

35. Zea CJ, Camci-Unal G, Pohl NL. Thermodynamics of binding of divalent magnesium and manganese to uridine phosphates: implications for diabetes-related hypomagnesaemia and carbohydrate biocatalysis. Chemistry Central J. 2008; 2:15.

36. Sinha SC, Wetterer M, Sprang SR, Schultz JE, Linder JU. Origin of asymmetry in adenylyl cyclases: structures of *Mycobacterium tuberculosis* Rv1900c. EMBO J. 2005; 24:663–673. [PubMed: 15678099]

37. Dessauer CW, Scully TT, Gilman AG. Interactions of forskolin and ATP with the cytosolic domains of mammalian adenylyl cyclase. J. Biol. Chem. 1997; 272:22272–22277. [PubMed: 9268376]

38. Suryanarayana S, Göttle M, Hübner M, Gille A, Mou T-C, Sprang SR, Richter M, Seifert R. Differential inhibition of various adenylyl cyclase isoforms and soluble guanylyl cyclase by 2',3'-*O*-(2,4,6-trinitrophenyl)-substituted nucleoside 5'-triphosphates. J. Pharmacol. Exp. Ther. 2009; 330:687–695. [PubMed: 19494187]

NIH-PA Author Manuscript
NIH-PA Author Manuscript
NIH-PA Author Manuscript

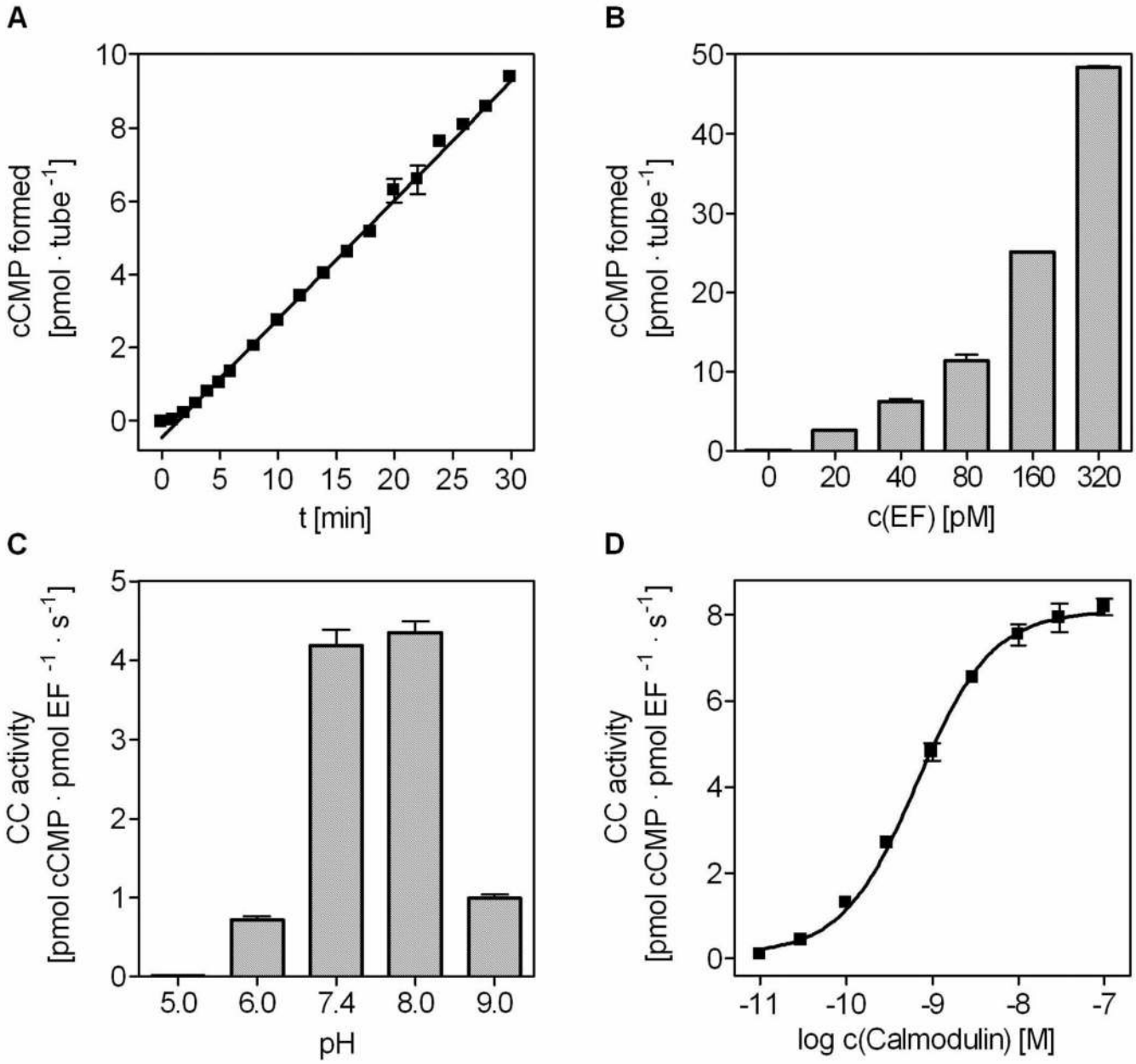

Fig. 1. Signals obtained using the isotopic EF cytidylyl cyclase activity assay

Reactions were carried out for 20 min at 37 °C as described in "Materials and Methods". **A:** Time course experiment using 20 pM EF. Reaction mixtures contained the following components to yield the given final concentrations: 100 mM KCl, 5 mM Mn^{2+}, 10 μM free Ca^{2+}, 100 μM EGTA, 10 μM CTP, [α–^{32}P]CTP (0.4 μCi/tube), 100 nM CaM. **B:** Signal dependence on EF protein concentration. Reaction mixtures contained EF at various concentrations, the components listed under A and additionally 100 μM cAMP. **C:** Dependence of CC activity on pH. Reaction mixtures contained 80 pM EF and the components listed under B. Buffering systems were 30 mM sodium acetate·HCl (pH 5.0 and pH 6.0), 30 mM Hepes·NaOH (pH 7.4) and 30 mM Tris·HCl (pH 8.0 and pH 9.0). **D:** Activation of CC activity by CaM. Reaction mixtures contained 5 mM Mn^{2+}, 10 μM free Ca^{2+}, 100 μM EGTA, 10 μM CTP, [α–^{32}P]CTP (0.4 μCi/tube), 40 pM EF and CaM at

various concentrations. Data shown are means ± SD of representative experiments performed in duplicates; similar results were obtained in at least 3 independent experiments.

NIH-PA Author Manuscript
NIH-PA Author Manuscript
NIH-PA Author Manuscript

NIH-PA Author Manuscript

NIH-PA Author Manuscript

NIH-PA Author Manuscript

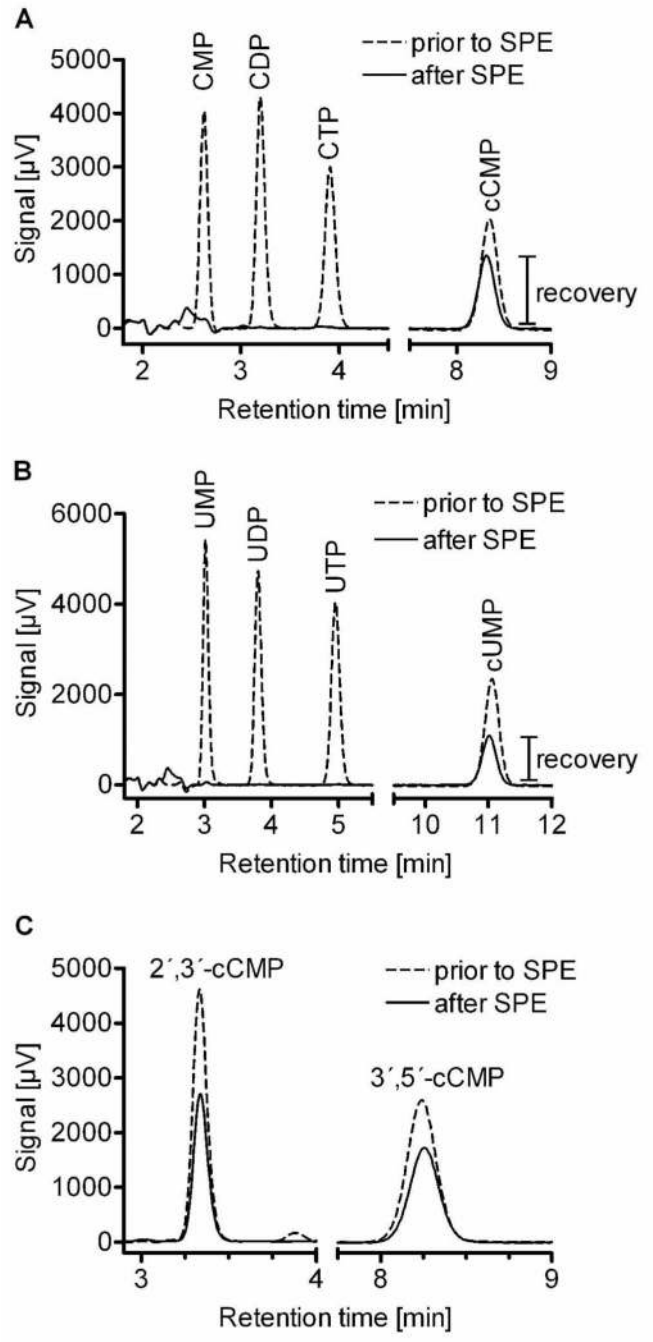

Fig. 2. HPLC chromatograms of nucleotide mixtures and eluates from solid phase extraction (SPE) using alumina

SPE and HPLC analytics were performed as described in "Materials and Methods". **A:** Chromatogram of a mixture of 15 µM CMP, CDP, CTP and 3′:5′-cCMP prior to SPE (dashed line) and chromatogram after SPE (solid line). **B:** Chromatogram of a mixture of 15 µM UMP, UDP, UTP and 3′:5′-cUMP prior to SPE (dashed line) and chromatogram after SPE (solid line). **C:** Chromatograms of 15 µM 2′:3′-cCMP and 3′:5′-cCMP prior to SPE (dashed line) and chromatogram after SPE (solid line). The same results were obtained in at least 3 independent experiments.

NIH-PA Author Manuscript

NIH-PA Author Manuscript

NIH-PA Author Manuscript

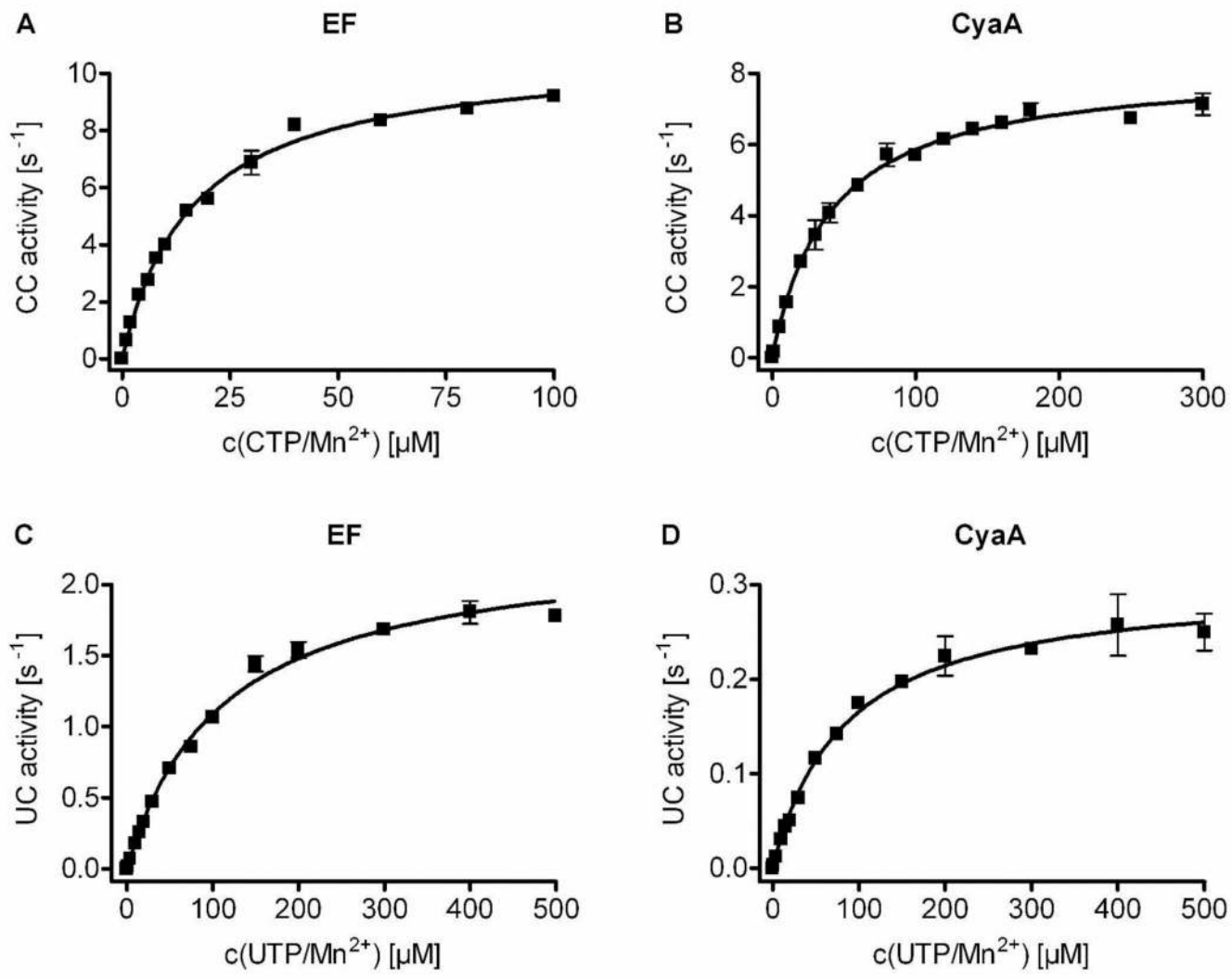

Fig. 3. Michaelis-Menten kinetics of CC and UC activity of EF and CyaA using the isotopic NC activity

Reactions were carried out as described in "Materials and Methods". Reaction mixtures contained the following components to yield the given final concentrations: 100 mM KCl, 10 μM free Ca^{2+}, 100 μM EGTA, [α–^{32}P]CTP (0.8 μCi/tube) or [α–^{32}P]UTP (0.8 μCi/tube), 100 nM CaM and non-labeled cyclic nucleotides as described in "Materials and Methods". CTP/Mn^{2+} or UTP/Mn^{2+} (1 μM to 1 mM) plus 5 mM of free Mn^{2+} were added. The final protein concentration was 40 pM EF or CyaA in case of CC activity (**A** and **B**) and 400 pM EF or CyaA in case of UC activity (**C** and **D**). Reactions were carried out at 37 °C for 20 min in case of CC activity and for 30 min in case of UC activity. Data shown are means ± SD of representative experiments performed in duplicates; similar results were obtained in at least 5 independent experiments.

NIH-PA Author Manuscript

NIH-PA Author Manuscript

NIH-PA Author Manuscript

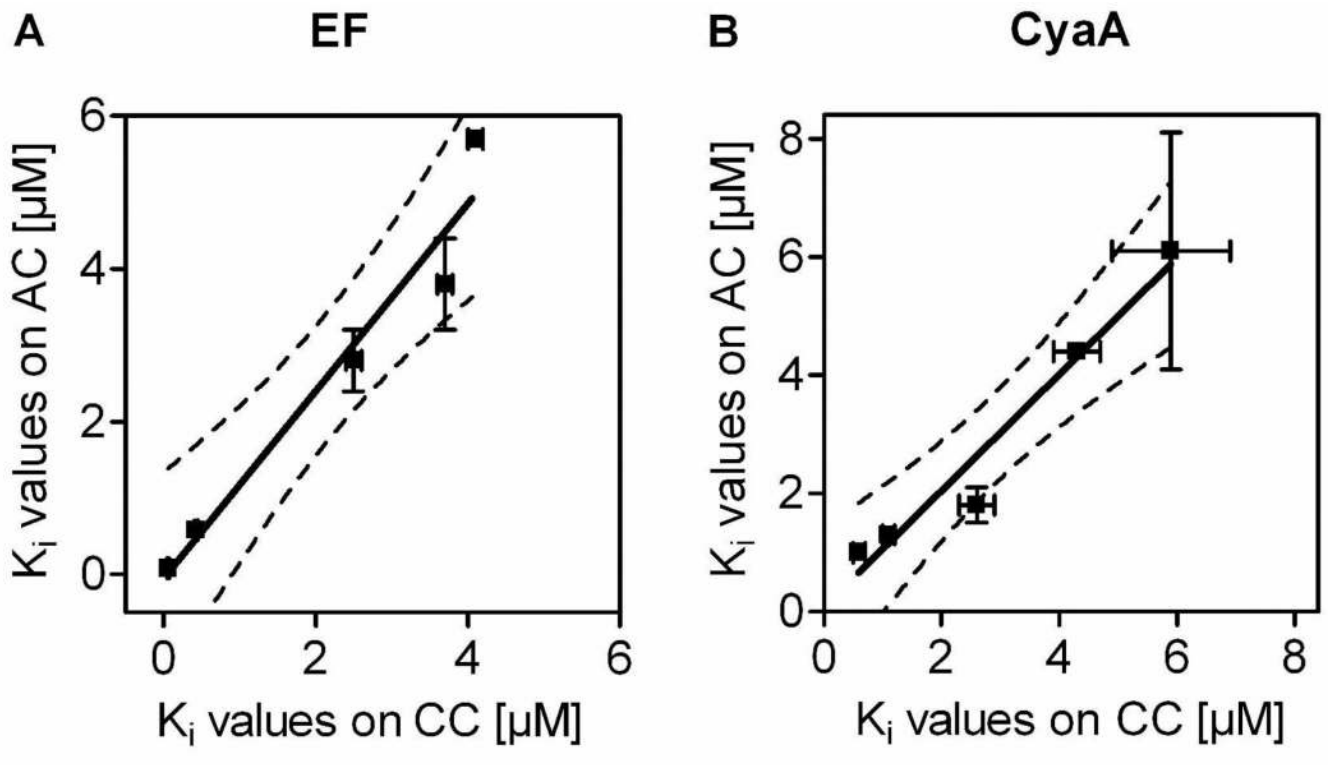

Fig. 4. Linear correlation of the K_i values of AC and CC inhibition by MANT-nucleotides

Data shown in Tab. **2** provide the basis for the correlations. Dashed lines represent 95% confidence intervals of the linear regression lines. **A:** Inhibition of EF; slope, 1.224 ± 0.1604; r^2, 0.9510; p, 0.0047; significant. **B:** Inhibition of CyaA; slope, 0.9847 ± 0.1226; r^2, 0.9555; p, 0.0040; significant. Linear regression analysis was performed using the Prism 4.02 software (Graphpad, San Diego, CA).

NIH-PA Author Manuscript

NIH-PA Author Manuscript

NIH-PA Author Manuscript

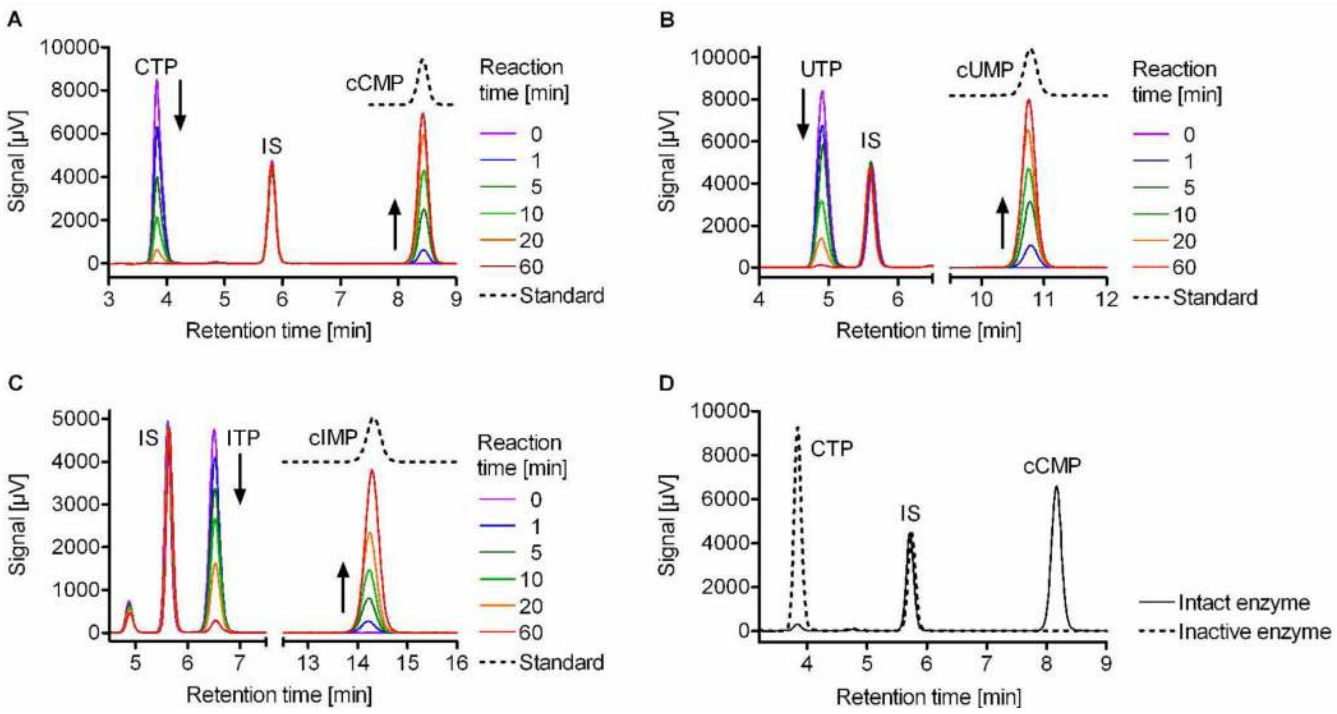

Fig. 5. HPLC chromatograms of reaction mixtures from the non-isotopic NC assay

The non-isotopic NC assay, sample preparation and HPLC analytics were carried out as described in "Materials and Methods". Reaction mixtures contained 5 mM Mn^{2+}, 5 µM Ca^{2+} and 100 µM CTP (**A**), UTP (**B**) or ITP (**C**). Protein concentrations were 20 nM EF and 20 nM CaM (A), 120 nM EF and 120 nM CaM (B) and 300 nM EF and 300 nM CaM (C). Samples were withdrawn at the indicated reaction times (colored solid lines). Inosine (20 µM) was added as internal standard (IS); cCMP, cUMP and cIMP were also added as standard substances (black, dotted lines). In order to prevent overlapping of the lines, the chromatograms of the standard substances were moved vertically. **D:** Chromatograms of reaction samples containing 20 nM EF, 20 nM CaM and 100 µM CTP after 60 min reaction time. Results for active enzyme (solid line) and heat-inactivated enzyme (dotted line). Similar results were obtained in at least 3 independent experiments.

NIH-PA Author Manuscript

NIH-PA Author Manuscript

NIH-PA Author Manuscript

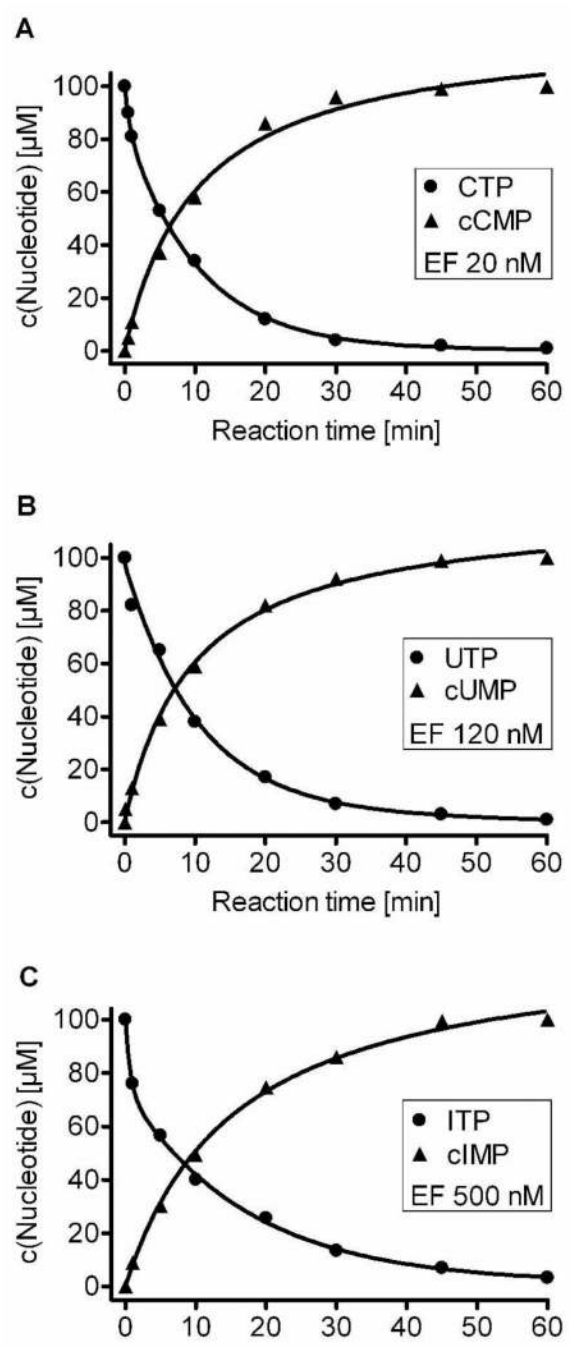

Fig. 6. Turnover of NTPs to cNMPs by EF using the non-isotopic NC assay

Nucleotide concentrations were calculated by evaluating the chromatograms shown in Fig. **5**. CTP (**A**), UTP (**B**) or ITP (**C**), 100 µM each, were converted to the corresponding cyclic nucleotides by the indicated concentrations of EF and equivalent concentrations of CaM ensuring 1:1 stoichiometry of EF and CaM. Experiments were performed as described in "Materials and Methods". Similar results were obtained in at least 3 independent experiments.

NIH-PA Author Manuscript

NIH-PA Author Manuscript

NIH-PA Author Manuscript

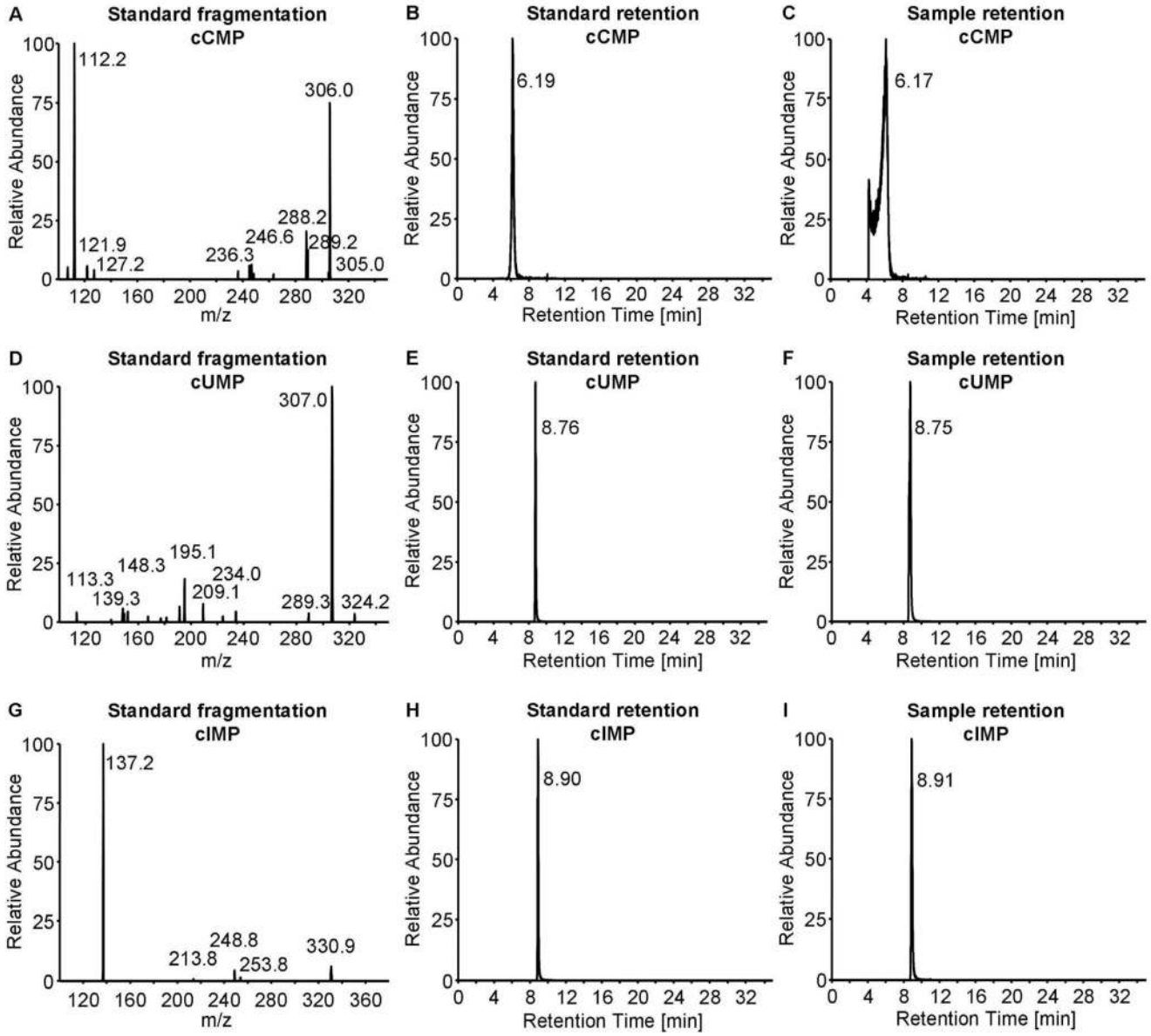

Fig. 7. Verification of the identities of the cyclic nucleotides formed in the non-isotopic NC assay by mass spectrometry

HPLC-MS analytics were performed as described in "Materials and Methods". Shown are fragmentation patterns of the standard cyclic nucleotides, chromatograms from standard cyclic nucleotides and chromatograms from reaction samples for cCMP (**A–C**), cUMP (**D–F**) and cIMP (**G–I**). Similar results were obtained in at least 3 independent experiments.

NIH-PA Author Manuscript
NIH-PA Author Manuscript
NIH-PA Author Manuscript

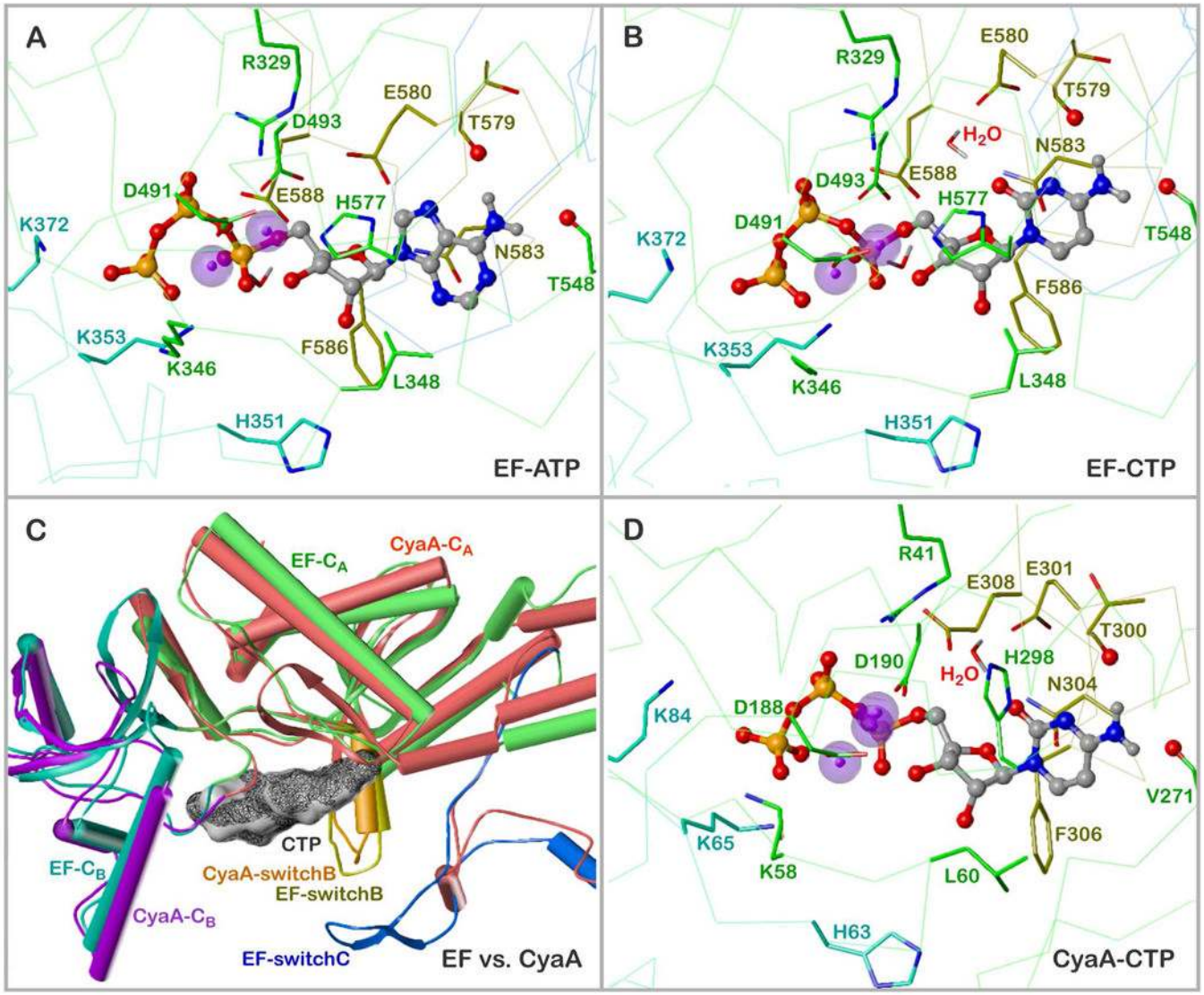

Fig. 8. Suggested interaction of nucleotides with EF and CyaA

The minimized models are based on the crystal structures of EF in complex with 3'-deoxy-ATP (28) and CyaA in complex with PMEApp (16), respectively. Colors of atoms, unless otherwise indicated: P – orange, O – red, N – blue, C, H –grey, Mg^{2+} – purple spheres. **A**, Interaction of EF with ATP. **B**, Interaction of EF with CTP. **C**, Alignment of the nucleotide binding sites of EF and CyaA in complex with CTP (represented as MOLCAD surfaces, bound to EF – black lines, bound to CyaA – grey opaque). Enzyme models: cylinders – helices, ribbons – β-sheets, tubes – loops, EF domain C_A – green, domain C_B – greenblue, switch B – yellow, switch C – blue, CyaA domain C_A – pink, domain B – purple, switch C_B – orange. **D**, Interaction of CTP with CyaA. In panels **A, B** and **D**, the side chains of the amino acids of the binding sites are drawn as sticks and labeled. Colors of C atoms and Cα-traces: domain A – green, domain B – greenblue, switch B – yellow. The backbone oxygen atoms suggested to form hydrogen bonds with the amino groups of ATP and CTP are marked as balls.

NIH-PA Author Manuscript
NIH-PA Author Manuscript
NIH-PA Author Manuscript

Table 1

Kinetic properties AC activities, CC activities and UC activities from EF and CyaA.

Enzyme	NC activity	Cation	K_m [μM]	k_{cat} [s^{-1}]	$k_{cat} \cdot K_m^{-1}$ [$M^{-1} \cdot s^{-1}$]
EF	**AC**	Mn^{2+}	35.3 ± 3.7	501.5 ± 55.9	$1{,}42 \cdot 10^7$
		Mg^{2+}	175.8 ± 29.9	684.2 ± 272.5	$3{,}89 \cdot 10^6$
	CC	Mn^{2+}	12.5 ± 3.4	8.8 ± 1.4	$7{,}04 \cdot 10^5$
		Mg^{2+}	419.7 ± 115.1	7.2 ± 3.1	$1{,}72 \cdot 10^4$
	UC	Mn^{2+}	134.5 ± 23.5	2.3 ± 0.2	$1{,}71 \cdot 10^4$
CyaA	**AC**	Mn^{2+}	57.7 ± 4.6	332.0 ± 42.4	$5{,}75 \cdot 10^6$
	CC	Mn^{2+}	46.6 ± 9.7	8.9 ± 2.0	$1{,}91 \cdot 10^5$
	UC	Mn^{2+}	68.6 ± 9.8	0.3 ± 0.05	$4{,}37 \cdot 10^3$

AC activities, CC activities and UC activities were determined as described under “Materials and Methods”. 1 μM to 2 mM NTP/Mn^{2+} or NTP/Mg^{2+} were added, plus 5 mM of free Mn^{2+} or Mg^{2+}. As radioactive tracer, [α-^{32}P]ATP (0.2 μCi/tube), [α-^{32}P]CTP (0.8 μCi/tube) or [α-^{32}P]UTP (0.8 μCi/tube) were added. The final enzyme concentrations were: 10 pM (EF and CyaA AC activities), 40 pM (EF and CyaA CC activities with Mn^{2+}), and 400 pM (EF CC activity with Mg^{2+} and UC activities). Reactions were carried out for 10 min at 25°C (AC), 20 min at 37°C (CC) and 30 min at 37°C (UC). Apparent K_m and K_{cat} values were obtained by non-linear regression analysis of substrate-saturation experiments and are the means ± SD of 3–4 independent experiments performed in duplicates. Saturation curves were analyzed by non-linear regression using the Prism 4.02 software (Graphpad, San Diego, CA).

Biochemistry. Author manuscript; available in PMC 2011 July 6.

NIH-PA Author Manuscript

NIH-PA Author Manuscript

NIH-PA Author Manuscript

Table 2

Inhibitor potencies at EF and CyaA AC and CC activities.

	K_i (μM)			
Nucleotide	**EF AC activity**	**EF CC activity**	**CyaA AC activity**	**CyaA CC activity**
MANT-ATP	0.43 ± 0.02	0.58 ± 0.03	4.3 ± 0.4***	4.4 ± 0.1
MANT-CTP	0.06 ± 0.01*	0.08 ± 0.01	1.1 ± 0.1***	1.3 ± 0.1
MANT-GTP	2.5 ± 0.1*	2.8 ± 0.4	5.9 ± 1.0***	6.1 ± 2.0
MANT-ITP	4.1 ± 0.1*	5.7 ± 0.03	0.6 ± 0.1***	1.0 ± 0.04
MANT-UTP	3.7 ± 0.1*	3.8 ± 0.6	2.6 ± 0.3***	1.8 ± 0.3

CC activities were determined as described under “Materials and Methods”. Reaction mixtures contained the following components to yield the given final concentrations: 100 mM KCl, 5 mM free Mn^{2+}, 10 μM free Ca^{2+}, 100 μM EGTA, 10 μM CTP, [α-^{32}P]CTP (0.4 μCi/tube), 100 μM cAMP, 100 nM CaM. The final protein concentration was 30 pM EF or CyaA, reactions were carried out for 20 min at 37°C.

Values labeled with (*) and (***) were taken from Ref. 29 and Ref. 26, respectively. Ki values are given in μM and represent the means ± SD of at least three independent experiments performed in duplicates. Inhibition curves were analyzed by non-linear regression using the Prism 4.02 software (Graphpad, San Diego, CA).